GLRT Based Scale-Invariant Multipolarization SAR Change Detection

V. Carotenuto*, C. Clemente†, A. De Maio*, and J. J. Soraghan†,
*Università degli Studi di Napoli "Federico II", DIETI, via Claudio 21, I-80125 Napoli, Italy
E-mail: vincenzo.carotenuto@unina.it, ademaio@unina.it
†University of Strathclyde, CESIP, EEE, 204, George Street, G1 1XW, Glasgow, UK
E-mail: carmine.clemente@strath.ac.uk, j.soraghan@strath.ac.uk

***Abstract*—The problem of coherent multi-polarization SAR change detection assuming the availability of image pairs, collected from N multiple polarimetric channels, is addressed in this paper. At the design stage, it is assumed that the reference and test images from the same polarimetric channel may exhibit a power mismatch. The change detection problem is formulated as a binary hypothesis testing problem, the principle of invariance is used to obtain the maximal invariant statistic, and the Generalized Likelihood Ratio Test (GLRT) is exploited to form a scale-invariant Constant False Alarm Rate (CFAR) decision rule. Results on real high resolution SAR data are provided that show the effectiveness of the proposed scale-invariant decision structures.**

I. Introduction

The ability to identify temporal changes within a given scene starting from a pair of co-registered SAR images representing an area of interest is a challenging SAR signal processing problem and is known as change detection [1], [2]. Two main approaches, known as incoherent and coherent, have been proposed in the literature to process the image pair. The former attempts to detect changes in the mean power level of a given scene exploiting only the images intensity information. The latter jointly use both amplitude and phase from the reference and the test data to detect possible changes.

Starting from the multi-polarization data model developed in [5] and [6], we generalize this model in this paper, accounting for a possible scale mismatch factor, and propose a new framework for change detection based on the theory of invariance in hypothesis testing problems [10], [11]. This is a viable means to force some desired properties to a decision statistic at the design stage and has already been successfully applied in some different radar detection problems [12], [13]. The principle of invariance allows us to focus on decision rules which exhibit some natural symmetries implying important practical properties such as the Constant False Alarm Rate (CFAR) behaviour. Furthermore, the use of invariance leads to a data reduction because all invariant tests can be expressed in terms of a statistic, called maximal invariant, which organizes the original data into equivalence classes. Also the parameter space is usually compressed after reduction by invariance and the dependence on the original set of parameters become embedded into a maximal invariant in the parameter space (induced maximal invariant). Furthermore, the new framework is able to produce a scale-invariant decision rule, providing advantages in terms of robustness and false alarm rejection. This is an important property as images over the same scene can exhibit different intensity scales due to different observation angles and propagation properties. These effects can lead to false alarms in a change detection framework that is not designed to be robust with respect to such a scale variations.

The remainder of the paper is organized as follows. In Section II, we deal with the formulation of the multi-polarization SAR change detection problem. In Section III the maximal invariant for the scale-invariant SAR change detection problem is defined. The scale invariant Generalized Likelihood Ratio Test (GLRT) detector is introduced in Section IV, and in Section V we assess the performance of the introduced invariant test on real multi-polarization SAR images. Finally, in Section VI, we draw conclusions.

A. Notation

We adopt the notation of using boldface for vectors and matrices. The transpose and conjugate transpose operators are denoted, respectively, by the symbols $(\cdot)^T$ and $(\cdot)^\dagger$. $\mathrm{tr}(\cdot)$ and $\det(\cdot)$ are respectively the trace and the determinant of the square matrix argument. $\boldsymbol{I}$ and $\mathbf{0}$ denote respectively the identity matrix and the matrix with zero entries (their size is determined from the context). $\mathbf{Diag}(\boldsymbol{a})$ indicates the diagonal matrix whose i-th diagonal element is the i-th entry of $\boldsymbol{a}$. The curled inequality symbol $\succ$ is used to denote generalized matrix inequality: for any Hermitian matrix $\boldsymbol{A}$, $\boldsymbol{A} \succ \mathbf{0}$ means that $\boldsymbol{A}$ is a positive definite matrix. The General Linear group of degree N over the field of complex numbers, denoted by $\mathcal{GL}(N)$, is the set of $N \times N$ non-singular matrices together with the operation of ordinary matrix multiplication. $\mathcal{H}_N^{++}$ and $\mathcal{R}^{++}$ denote, respectively, the set of $N \times N$ Hermitian positive definite matrices and the set of positive real numbers. $\mathbf{1}_N$ is the $1 \times N$ vector with all the entries equal to one.

II. Problem Formulation

A multipolarization SAR sensor measures, for each pixel of the image under test, $N \in \{2, 3\}$ complex returns, collected from different polarimetric channels (for instance HH and VV for $N = 2$; HH, VV, and HV with reference to $N = 3$). The N returns from the same pixel are stacked to form the vector $\boldsymbol{X}(l, m)$, where $l = 1, \dots, L$ and $m = 1, \dots, M$ (L and M represent the vertical and horizontal size of the image, respectively). Therefore, the sensor provides a 3-D data stack $\boldsymbol{X}$ of size $M \times L \times N$ which will be referred to in the following as the "datacube".

For SAR change detection applications, we assume that two datacubes $\boldsymbol{X}$ (reference data) and $\boldsymbol{Y}$ (test data) of the same geographic area are available. Furthermore it is assumed

978-1-4799-4195-7/14/$31.00©2014IEEE

that they are collected from two different sensor passes and are accurately pixel aligned (co-registered). We focus on the problem of detecting the presence of possible changes in a rectangular neighbourhood $\mathcal{A}$, with size $K = W_1 \times W_2 \geq 3$, of a given pixel. To this end, we denote by $\boldsymbol{R}_X$ ($\boldsymbol{R}_Y$) the matrix whose columns are the vectors of the polarimetric returns from the pixels of $\boldsymbol{X}$ ($\boldsymbol{Y}$) which fall in the region $\mathcal{A}$ with $\boldsymbol{S}_X = \boldsymbol{R}_X \boldsymbol{R}_X^\dagger$ and $\boldsymbol{S}_Y = \boldsymbol{R}_Y \boldsymbol{R}_Y^\dagger$.

The matrices $\boldsymbol{R}_X$ and $\boldsymbol{R}_Y$ are modelled as statistically independent random matrices. Moreover, the columns of $\boldsymbol{R}_X$ and $\boldsymbol{R}_Y$ are assumed statistically independent and identically distributed random vectors drawn from a complex circular zero-mean Gaussian distribution with positive definite covariance matrix $\boldsymbol{\Sigma}_X$ and $\boldsymbol{\Sigma}_Y$ respectively. Under the aforementioned settings, the change detection problem in the region $\mathcal{A}$ can be formulated in terms of the following binary hypothesis test

$$\begin{cases} H_0 : \boldsymbol{\Sigma}_X = \gamma \boldsymbol{\Sigma}_Y \\ H_1 : \boldsymbol{\Sigma}_X \neq \gamma \boldsymbol{\Sigma}_Y \end{cases} \tag{1}$$

where the null hypothesis H_0 of change absence is tested versus the alternative H_1 accounting for the parameter $\gamma > 0$ that models possible received power variations between two different acquisitions from the same scene, due to not perfectly aligned flight paths as well as channel propagation effects.

Exploiting the Gaussian assumption, we can write the joint probability density function (pdf) of $\boldsymbol{R}_X$ and $\boldsymbol{R}_Y$ as

$$f_{\boldsymbol{R}_X,\boldsymbol{R}_Y}(\boldsymbol{R}_X, \boldsymbol{R}_Y | H_1, \boldsymbol{\Sigma}_X, \boldsymbol{\Sigma}_Y) = \frac{1}{\pi^{2NK} \det(\boldsymbol{\Sigma}_X \boldsymbol{\Sigma}_Y)^K} \exp\left\{-\mathrm{tr}\left(\boldsymbol{\Sigma}_X^{-1} \boldsymbol{S}_X + \boldsymbol{\Sigma}_Y^{-1} \boldsymbol{S}_Y\right)\right\} . \tag{2}$$

Using the Fisher-Neyman factorization theorem [15], we can claim that a sufficient statistic for (1) is represented by the two sample Grammian matrices $\boldsymbol{S}_X$ and $\boldsymbol{S}_Y$ which are statistically independent and follow a complex Wishart distribution, i.e.

$$f_{\boldsymbol{S}_X}(\boldsymbol{S}_X | H_1, \boldsymbol{\Sigma}_X) = \frac{c_W}{\det(\boldsymbol{\Sigma}_X)^K} \exp\left\{-\mathrm{tr}\left(\boldsymbol{\Sigma}_X^{-1} \boldsymbol{S}_X\right)\right\} \det(\boldsymbol{S}_X)^{K-N}, \quad \boldsymbol{S}_X \succ \boldsymbol{0} \tag{3}$$

$$f_{\boldsymbol{S}_Y}(\boldsymbol{S}_Y | H_1, \boldsymbol{\Sigma}_Y) = \frac{c_W}{\det(\boldsymbol{\Sigma}_Y)^K} \exp - \left\{\mathrm{tr}\left(\boldsymbol{\Sigma}_Y^{-1} \boldsymbol{S}_Y\right)\right\} \det(\boldsymbol{S}_Y)^{K-N}, \quad \boldsymbol{S}_Y \succ \boldsymbol{0} \tag{4}$$

with c_W a normalization constant. From the sufficient statistic we can evaluate the optimum Neyman-Pearson (NP) detector as the Likelihood Ratio Test (LRT), which, after standard algebra and statistical equivalences, can be expressed as

$$\mathrm{tr}\left[\left(\frac{\boldsymbol{\Sigma}_Y^{-1}}{\gamma} - \boldsymbol{\Sigma}_X^{-1}\right) \boldsymbol{S}_X\right] \underset{H_0}{\overset{H_1}{\gtrless}} T_0 \tag{5}$$

where T_0 is the detection threshold. Evidently, test (5) is not Uniformly Most Powerful (UMP) and, consequently, it is not practically implementable because it requires the knowledge of $\boldsymbol{\Sigma}_X$, γ, and $\boldsymbol{\Sigma}_Y$ which, in realistic applications, are usually unknown.

III. Data Reduction and Invariance Issues

Both hypotheses under test are composite or, otherwise stated, H_0 and H_1 are equivalent to a partition of the parameter space Θ into the two disjoint sets

$$\begin{aligned} \Theta_0 &= \left\{\boldsymbol{\Sigma}_X = \gamma \boldsymbol{\Sigma}_Y,\ (\boldsymbol{\Sigma}_X, \boldsymbol{\Sigma}_Y, \gamma) \in \mathcal{H}_N^{++} \times \mathcal{H}_N^{++} \times \mathcal{R}^{++}\right\} \\ \Theta_1 &= \left\{\boldsymbol{\Sigma}_X \neq \gamma \boldsymbol{\Sigma}_Y,\ (\boldsymbol{\Sigma}_X, \boldsymbol{\Sigma}_Y, \gamma) \in \mathcal{H}_N^{++} \times \mathcal{H}_N^{++} \times \mathcal{R}^{++}\right\} \end{aligned} \tag{6}$$

This formulation emphasizes that the individual values of the nuisance parameters are irrelevant: one must only decide which hypothesis is valid, namely whether the covariances are proportional or not. This remark suggests that we can cluster the data considering transformations that leave the following unaltered:

a. the two composite hypotheses, namely the partition of the parameter space;

b. the families of distributions under the two hypotheses.

This goal can be achieved through the *Principle of Invariance* [11]. According to this principle, we look for transformations that preserve the formal structure of the hypothesis testing problem and, then, we derive decision rules invariant to them. Such a principle also acts as a data reduction technique leading to a reduced observation space of significantly lower dimensionality than the original one.

It is not difficult to prove that our testing problem is invariant under the group of transformations G acting on the sufficient statistic as:

$$G = \Big\{ g : \boldsymbol{S}_X \to \boldsymbol{B}\boldsymbol{S}_X\boldsymbol{B}^\dagger, \quad \boldsymbol{S}_Y \to a\boldsymbol{B}\boldsymbol{S}_Y\boldsymbol{B}^\dagger, \quad \boldsymbol{B} \in \mathcal{GL}(N), \quad a \in \mathcal{R}^{++} \Big\} \tag{7}$$

In fact, the families of distributions are preserved because if $\boldsymbol{S}_X$ and $\boldsymbol{S}_Y$ are Wishart distributed then $\boldsymbol{B}\boldsymbol{S}_X\boldsymbol{B}^\dagger$ and $\boldsymbol{B}\boldsymbol{S}_Y\boldsymbol{B}^\dagger$ are also Wishart with the same scalar parameters and matrix parameter $\boldsymbol{B}^\dagger \boldsymbol{\Sigma}_X \boldsymbol{B}$ and $a\boldsymbol{B}^\dagger \boldsymbol{\Sigma}_Y \boldsymbol{B}$, where $\boldsymbol{B} \in \mathcal{GL}(N)$ and $a > 0$. Moreover, the original partition of the parameter space is left unaltered since if $\boldsymbol{\Sigma}_X \neq \gamma \boldsymbol{\Sigma}_Y$ then $\boldsymbol{B}\boldsymbol{\Sigma}_X\boldsymbol{B}^\dagger \neq a\gamma \boldsymbol{B}\boldsymbol{\Sigma}_Y\boldsymbol{B}^\dagger$ and if $\boldsymbol{\Sigma}_X = \gamma \boldsymbol{\Sigma}_Y$ then $\boldsymbol{B}\boldsymbol{\Sigma}_X\boldsymbol{B}^\dagger = a\gamma_1 \boldsymbol{B}\boldsymbol{\Sigma}_Y\boldsymbol{B}^\dagger$.

A. Maximal Invariant Design

The invariance property induces a partition of the data space into orbits (or equivalence classes) where, over each orbit, every point is related to every other through a transformation which is a member of the group G. Any statistic that identifies different orbits in a one-to-one way significantly reduces the total amount of data necessary for solving the hypothesis testing problem and constitutes the compressed data set to be used in the design of any invariant detector. These kind of statistics are called maximal invariants since they are constant over each orbit (invariance) while they assume different values on different orbits (maximality).

Formally, a statistic $\mathbf{T}(\boldsymbol{S}_X, \boldsymbol{S}_Y)$ is said to be a maximal invariant with respect to the group of transformations G if and only if

- Invariance:
  $\mathbf{T}(\boldsymbol{S}_X, \boldsymbol{S}_Y) = \mathbf{T}[g(\boldsymbol{S}_X, \boldsymbol{S}_Y)]$, $\forall g \in G$.

- Maximality:
  $\mathbf{T}(\boldsymbol{S}_{X_1}, \boldsymbol{S}_{Y_1}) = \mathbf{T}(\boldsymbol{S}_{X_2}, \boldsymbol{S}_{Y_2})$ implies that $\exists g \in G$ such that $(\boldsymbol{S}_{X_2}, \boldsymbol{S}_{Y_2}) = g(\boldsymbol{S}_{X_1}, \boldsymbol{S}_{Y_1})$.

Notice that there are many maximal invariant statistics, but they are equivalent in that yield statistically equivalent detectors. Moreover, all invariant tests can be expressed as a function of the maximal invariant statistic [10], which for the problem of interest is provided by the following proposition

Proposition 1: A maximal invariant statistic for problem (1) with respect to the group of transformations (7) is the $(N-1)$-dimensional vector

$$\left(\frac{\lambda_2}{\lambda_1}, \frac{\lambda_3}{\lambda_1}, \ldots, \frac{\lambda_N}{\lambda_1}\right) \tag{8}$$

where $\lambda_1 \geq \lambda_2 \geq, \ldots, \geq \lambda_N$ are the eigenvalues of $\boldsymbol{S}_X \boldsymbol{S}_Y^{-1}$.

Interestingly the principle of invariance realizes a significant data reduction: the maximal invariant statistic is a real N-dimensional vector whereas the original sufficient statistic comprises two $N \times N$ Grammian matrices $\boldsymbol{S}_X$ and $\boldsymbol{S}_Y$.

B. Induced Maximal Invariant Design

The data transformation induces a parameter transformation which leaves unaltered the two composite hypotheses. In other words, by the principle of invariance, the parameter space is also partitioned into orbits which usually results in a reduced set of parameters. The relevant parameters are embodied into an *induced maximal invariant*, namely any function of the parameters that is constant over each orbit of the parameter space (invariance) but assumes different values over different orbits (maximality).

For the case at hand, an induced maximal invariant is composed of $\left(\frac{\delta_2}{\delta_1}, \ldots, \frac{\delta_N}{\delta_1}\right)$, where $\boldsymbol{\delta} = [\delta_1, \ldots, \delta_N]^T$ are the eigenvalues of the matrix:

$$\boldsymbol{\Sigma}_X \boldsymbol{\Sigma}_Y^{-1} \,. \tag{9}$$

The previous claim highlights that the principle of invariance yields also a significant reduction of the number of the parameters: in fact, the induced maximal invariant is an $(N-1)$-dimensional vector while the original parameter space was composed of the two covariance matrices $\boldsymbol{\Sigma}_X$, $\boldsymbol{\Sigma}_Y$ and γ.

We explicitly observe that in the reduced parameter space the partition corresponding to the two composite hypotheses of the test (1) is $\Xi_0 = \{\mathbf{1}_{N-1}\}$, relative to $\boldsymbol{\Sigma}_X = \gamma\boldsymbol{\Sigma}_Y$, and $\Xi_1 = \overline{\{\mathbf{1}_{N-1}\}}$, relative to $\boldsymbol{\Sigma}_X \neq \gamma\boldsymbol{\Sigma}_Y$, where $\overline{\{\mathbf{1}_{N-1}\}}$ is the set of the $(N-1)$-dimensional column vectors with positive elements and at least one entry different from 1. The structure of Ξ_0, which now corresponds to a simple H_0 hypothesis, clearly shows that all invariant receivers that process a maximal invariant statistic through a transformation independent of $\left(\frac{\delta_2}{\delta_1}, \ldots, \frac{\delta_N}{\delta_1}\right)$, achieve the CFAR property.

IV. GLRT Derivation

This section derives the GLRT detector for the considered problem. Precisely, the decision rule (10) is considered, which, after the optimizations over $\boldsymbol{\Sigma}_X$ and $\boldsymbol{\Sigma}_Y$ at the numerator and over $\boldsymbol{\Sigma}_Y$ at the denominator can be recast (after some algebra and statistical equivalences) as,

$$\frac{\min\limits_{\gamma>0}\left[\gamma^N \det^2\left(\frac{\boldsymbol{S}_X}{\gamma} + \boldsymbol{S}_Y\right)\right]}{\det(\boldsymbol{S}_X)\det(\boldsymbol{S}_Y)} \underset{H_0}{\overset{H_1}{\gtrless}} T_1 \,, \tag{11}$$

or equivalently as

$$\frac{\min\limits_{\gamma>0}\left[\gamma^N \det^2\left(\frac{\boldsymbol{S}_Y^{-\frac{1}{2}}\boldsymbol{S}_X\boldsymbol{S}_Y^{-\frac{1}{2}}}{\gamma} + \boldsymbol{I}\right)\right]}{\det(\boldsymbol{S}_Y^{-\frac{1}{2}}\boldsymbol{S}_X\boldsymbol{S}_Y^{-\frac{1}{2}})} \underset{H_0}{\overset{H_1}{\gtrless}} T_1, \tag{12}$$

where T_1 is a suitable modification of the original threshold in (10). In order to proceed further we have to distinguish between the cases of two ($N = 2$) and three ($N = 3$) polarimetric channels.

A. Case $N = 2$

Forcing $N = 2$ in (11) yields

$$\frac{\min\limits_{\gamma>0}\left[\gamma^2\left(\frac{\lambda_1}{\gamma}+1\right)^2\left(\frac{\lambda_2}{\gamma}+1\right)^2\right]}{\lambda_1\lambda_2} \underset{H_0}{\overset{H_1}{\gtrless}} T_1 \,. \tag{13}$$

It is now necessary to compute

$$\min_{\gamma>0}\left[\frac{1}{\gamma}\left(\lambda_1\lambda_2 + \gamma^2 + (\lambda_1+\lambda_2)\gamma\right)\right]^2 . \tag{14}$$

Standard arguments on optimization of univariate functions provides the optimal point $\gamma_{opt,2} = \sqrt{\lambda_1\lambda_2}$. As a consequence, the GLRT becomes

$$\left(\sqrt{\frac{\lambda_1}{\lambda_2}}+1\right)^2\left(\sqrt{\frac{\lambda_2}{\lambda_1}}+1\right)^2 \underset{H_0}{\overset{H_1}{\gtrless}} T_1 \,. \tag{15}$$

Observing that the left hand side of (15) is a monotone increasing function of $\sqrt{\frac{\lambda_1}{\lambda_2}}$ for $\sqrt{\frac{\lambda_1}{\lambda_2}} \in [1, +\infty[$, the GLRT (15) turns out to be equivalent to

$$\frac{\lambda_1}{\lambda_2} \underset{H_0}{\overset{H_1}{\gtrless}} T_2 \,, \tag{16}$$

with T_2 the modified threshold. Two important comments are now in order. First, test (16) is equivalent to comparing the condition number of the matrix $\boldsymbol{S}_Y^{-\frac{1}{2}}\boldsymbol{S}_X\boldsymbol{S}_Y^{-\frac{1}{2}}$ with a detection threshold to establish the presence of changes in the considered scene. Second, the GLRT statistic is a maximal invariant.

V. Testing on Real Data

In this section the performance analysis on real X-band data is presented. The dataset used is the Coherent Change Detection Challenge dataset acquired by the Air Force Research Laboratory (AFRL) [14], the data contains passes acquired with three polarizations (HH, VV and HV).

For our analysis we focus on two acquisitions from the

$$\frac{\max\limits_{\boldsymbol{\Sigma}_X}\max\limits_{\boldsymbol{\Sigma}_Y} \frac{1}{(\pi)^{2NK}\det^K(\boldsymbol{\Sigma}_X)\det^K(\boldsymbol{\Sigma}_Y)} \exp\left[-\mathrm{tr}\left(\boldsymbol{\Sigma}_X^{-1}\boldsymbol{S}_X + \boldsymbol{\Sigma}_Y^{-1}\boldsymbol{S}_Y\right)\right]}{\max\limits_{\gamma>0}\max\limits_{\boldsymbol{\Sigma}_Y} \frac{1}{(\pi)^{2NK}\gamma^{NK}\det^{2K}(\boldsymbol{\Sigma}_Y)} \exp\left[-\mathrm{tr}\left(\boldsymbol{\Sigma}_Y^{-1}\left(\frac{\boldsymbol{S}_X}{\gamma} + \boldsymbol{S}_Y\right)\right)\right]} \underset{H_0}{\overset{H_1}{\gtrless}} T\,, \tag{10}$$

entire dataset, unfortunately the ground truths of the data is not available (e.g. the actual changes between two different acquisitions), so the selection of two passes providing the opportunity to generate a sufficiently accurate ground truth was required. For this reason the best candidates result to be two passes: the acquisition named "FP0124" is used as reference pass, while the acquisition "FP0121" is used as test pass. The selected area of interest is a sub-image of 1000×1000 pixels (i.e., $L = M = 1000$) and is composed of several parking lots which are occupied by numerous parked, (i.e., stationary) vehicles. For this particular scenario the changes between the reference and test images (denoted by $\boldsymbol{X}$ and $\boldsymbol{Y}$ respectively), occurred during the time interval between the two acquisitions can be distinguished in two cases:

- a vehicle is present in $\boldsymbol{X}$ but is not present in $\boldsymbol{Y}$, this case is referred as departure;
- a vehicle is not present in $\boldsymbol{X}$ but is present in $\boldsymbol{Y}$, this event is referred as arrival.

Using the cases defined above, a total of 34 changes between $\boldsymbol{X}$ and $\boldsymbol{Y}$ can be visually identified (by flickering the two images). The obtained ground truth is shown in Figure 1-a, wherein the black rectangle represent departures and the white rectangles indicate arrivals.

Although the acquisitions were performed during the same day and the images were registered, the returns from a scatterer can contribute differently to neighbour pixels, for example a slightly different aspect angle can produce a different amount of energy spill-over. These relative differences in the imaged data can lead to false alarms in the change detection results. For this reason we consider a guard area around each arrival-departure. This allows the definition of an extended ground truth (see Figure 1-b) used in the following to compare the performance of the considered detection algorithms.

In order to assess the performance of the detectors we

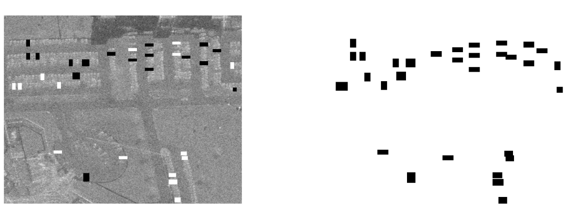

(a) Ground truth. (b) Ground truth with guard cells.

Fig. 1: Ground truth superimposed to the reference image and ground truth with the addition of guard cells.

present both the a-posteriori false alarm probability and the change detection maps for the case $N = 2$, (detector (16)). In the first analysis the thresholds are set to ensure $P_{fa} = 10^{-4}$, the thresholds have been obtained via Monte-Carlo simulations. In Table I the a-posteriori false alarm probability for (16) and the detectors (7), (10), (11), and (12) in [18] are reported. These values are estimated by applying a scaling α to the reference image, in particular values of α equal to 1, 1.5 and 2 were considered.

Table I shows how detector (16) provides constant false alarm probability despite the scale variation (possibly due to a non-perfect calibration)of the images for both the $W = 3$ and $W = 5$ cases.

In the second analysis the detector (16) has been tested by imposing $P_{fa} = 10^{-3}$ and with $W = 5$, on scaled version of the test image α equal to 1, 1.5 and 2. An example of detection map for $\alpha = 1$, $W = 5$ and $N = 2$ is shown in Figure 2. For all the three analysed cases the detection maps resulted to be identical with 2184 detections in total of which 1223 resulted to be actual changes, as expected from the scale invariance of the proposed approach.

		Detector				
W	α	(7) in [18]	(10) in [18]	(11) in [18]	(12) in [18]	(16)
3	1	0.039	0.041	0.030	0.046	0.044
	1.5	0.081	0.079	0.077	0.078	0.044
	2	0.212	0.177	0.199	0.218	0.044
5	1	0.077	0.077	0.065	0.079	0.063
	1.5	0.330	0.189	0.281	0.342	0.063
	2	0.981	0.653	0.948	0.982	0.063

TABLE I: False alarm probability for the case $N = 2$ on real data, detector (16) compared with those proposed in [18].

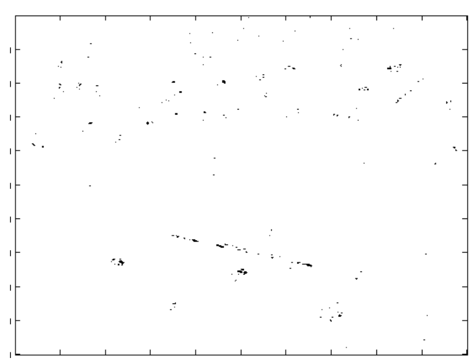

Fig. 2: Detection map for $\alpha = 1$, $W = 5$ and $N = 2$.

VI. Conclusions

Multi-polarization scale-invariant SAR change detection has been considered in this paper. The problem has been formulated as a binary hypothesis test and the principle of invariance has been applied to design decision rules. The GLRT detector for the case of two polarizations has been derived and tested on real SAR data in this paper. In a future work the case of full polarimetric data will be addressed applying the same framework.

REFERENCES

[1] M. Preiss and N. J. S. Stacy, "Coherent Change Detection: Theoretical Description and Experimental Results", Intelligence, Surveillance and Reconnaissance Division, Defence Science and Technology Organisation, DSTO-TR-1851.

[2] R. Touzi, A. Lopes, J. Bruniquel, and P. W. Vachon, "Coherence Estimation for SAR Imagery", IEEE Trans. Geosci. Remote Sens., vol. 37, no. 1, pp. 135-149, Jan. 1999.

[3] I. Stojanovic and L. Novak, "Algorithms Improve Synthetic Aperture Radar Coherent Change Detection Performance", SPIE Newsroom. doi: 10.1117/2.1201307.004889, Jul. 2013.

[4] E. J. M. Rignot and J. J. Van Zyl, "Change Detection Techniques for ERS-1 SAR data", IEEE Trans. Geosci. Remote Sens., vol. 31, no. 4, pp. 896-906, Jul. 1993.

[5] K. Conradsen, A. A. Nielsen, J. Schou, and H. Skriver, "A Test Statistic in the Complex Wishart Distribution and Its Application to Change Detection in Polarimetric SAR Data", IEEE Trans. Geosci. Remote Sens., vol. 41, no. 1, pp. 4-19, Jan. 2003.

[6] L. M. Novak, "Change Detection for Multi-polarization, Multi-pass SAR", SPIE Conference on Algorithms for Synthetic Aperture Radar Imagery XII, Orlando, FL, pp. 234-246, March 2005.

[7] A. A. Nielsen, R. Larsen, and H. Skriver, "Change Detection in Bi-Temporal EMISAR data from Kalø, Denmark, by means of canonical correlations analysis", in Proc. 3rd Int. Airborne Remote Sensing Conf. and Exhibition, Copenhagen, Denmark, July 7-10, 1997.

[8] A. A. Nielsen, "Change detection in multispectral bi-temporal spatial data using orthogonal transformations", in Proc. 8th Austral-Asian Sensing Conf., Canberra ACT, Australia, Mar. 25-29, 1996.

[9] E. Erten, A. Reigber, L. Ferro-Famil, and O. Hellwich, "A New Coherent Similarity Measure for Temporal Multichannel Scene Characterization", IEEE Trans. Geosci. Remote Sens., vol. 50, no. 7, pp. 2839-2851, Jul. 2012.

[10] R. J. Muirhead, "Aspects of Multivariate Statistical Theory", Wiley, New York (1982).

[11] E. L. Lehmann, "Testing Statistical Hypotheses", Springer-Verlag, 2nd edition, 1986.

[12] A. De Maio and E. Conte, "Adaptive Detection in Gaussian Interference With Unknown Covariance After Reduction by Invariance", IEEE Trans. on Signal Processing, Vol. 58, no. 6, pp. 2925-2934, Jun. 2010.

[13] E. Conte, A. De Maio, and C. Galdi, "CFAR Detection of Multi-dimensional Signals: an Invariant Approach", IEEE Trans. on signal processing, Vol. 58, no. 1, p. 142-151, Jan. 2003.

[14] U.S. Air Force Sensor Data Management System, "Coherent Change Detection Challenge Problem", https://www.sdms.afrl.af.mil/index.php?collection=ccd_challenge.

[15] S. M. Kay, "Fundamentals of Statistical Signal Processing: Estimation Theory", Vol. I, Prentice-Hall PTR, 1998.

[16] R. A. Horn and C. R. Johnson, *Matrix Analysis*, Cambridge, MA: Cambridge Univ. Press, 1985.

[17] H. L. Van Trees, "Detection, Estimation, and Modulation Theory", Pt. 1, John Wiley & Sons, 1968.

[18] V. Carotenuto, A. De Maio, C. Clemente, and J. J. Soraghan, "Multi-Polarization SAR Change Detection with Invariant Decision Rules", Submitted to IEEE RadarCon 2014, Cincinnati.